Bull. Chem. Soc. Jpn., 70, 71—78 (1997)

Photoemission Cross Sections for Ions Produced by Collisions of $He(2^3S)$ Atoms with Linear Triatomic Molecules and Fluorobenzenes

Ikuo Tokue,* Takeyuki Kudo, Masaaki Kobayashi, and Katsuyoshi Yamasaki

Department of Chemistry, Faculty of Science, Niigata University, Ikarashi, Niigata 950-21

(Received July 25, 1996)

Photoemissions at 200—650 nm resulting from the $He(2^3S)$ Penning ionization of CO_2, CS_2, OCS, N_2O, C_6F_6, and C_6F_5H have been studied in the collision energy range of 120—210 meV using a crossed-beam method. The emission cross sections obtained for the excited parent ions were compared with the values measured at thermal energy. The band strengths for the vibrational bands of the $OCS^+(\tilde{A}–\tilde{X})$ system are rather different from the values measured by the photoionization of OCS. The dependences of the emission cross sections for triatomic ions on the collision energy have been compared with those of the partial cross sections for the ion states obtained by Penning ionization electron spectroscopy, and the interaction potentials between $He(2^3S)$ and the triatomic molecules correlating with the Penning ionization are discussed.

The helium metastable atom $He(2^3S)$ can ionize simple molecules to some electronically excited states (Penning ionization), since its available energy (19.82 eV) is larger than the ionization potentials of the valence electrons of the target molecules. The mechanism of the Penning ionization of $He(2^3S)$ atom has been experimentally studied by electron spectroscopy (PIES) and optical spectroscopy (PIOS). In PIES, kinetic energy distributions[1] and angular dependence[2] of ejected electrons, and the values of the energy shift[3] have been studied. These data provide information concerning the interaction potentials of the entrance and exit channels. In PIOS we determine the emission rate constants or emission cross sections (σ_{em}) of electronically excited ions and the internal energy distributions of the product ions in order to study energy-partition process.[4,5]

PIOS studies on diatomic and polyatomic molecules in the thermal energy region have been carried out using a flowing afterglow (FA) method[5] operated at relatively high pressures of the buffer gas. Unfortunately, the application of the FA method to measurements at higher energy seems to be difficult. We have thus developed a crossed-beam method.[6] This technique enables us to study the dependence of the state-resolved cross sections for the formation of excited ions having a collision energy of up to 400 meV.[7] The dependence can provide information about the type of interaction between the metastable atoms and the target molecules and about the ionization dynamics.[8]

The Penning ionization of CO_2 with $He(2^3S)$ was studied by PIES[3,9—11] and PIOS.[12,13] Wauchop and Broida[12a] as well as Endoh et al.[13] determined the emission rate constants of the $CO_2^+(\tilde{A}^2\Pi_u–\tilde{X}^2\Pi_g)$ and $CO_2^+(\tilde{B}^2\Sigma_u^+–\tilde{X}^2\Pi_g)$ bands, and evaluated the branching ratio of the A and B states of CO_2^+. These ratios obtained by PIOS, however, are apparently larger than the PIES data.[3,10] This discrepancy is ascribed to a crossover from the B state to the A state via intermolecular processes.[13] The reactions of $He(2^3S)$ with CS_2 were studied by the FA method.[14,15] Yencha and Wu[15] observed the $CS(B^1\Sigma^+–A^1\Pi)$ band, while the spectroscopic constants obtained by several researchers[16] were contrary to their assignments. The reactions of $He(2^3S)$ with OCS were studied by the FA method.[17,18] Tsuji et al.[18] obtained the emission rate constant of the $OCS^+(\tilde{A}^2\Pi–\tilde{X}^2\Pi)$ transition. Chang et al.[19] measured the emission rate constants of the B–X band of the parent ions resulting from the $He(2^3S)$ Penning ionization of fluorobenzenes. Nevertheless, there has been only a little amount of information on the cross sections for the formation of electronically excited ions resulting from the reaction of $He(2^3S)$ with these target molecules, especially above the thermal energy.

In a preliminary study,[6] σ_{em} for the $N_2O^+(\tilde{A}^2\Sigma^+–\tilde{X}^2\Pi)$ band, resulting from the $He(2^3S)$ Penning ionization of N_2O, was measured at an impact energy of 150 meV. In the present paper, we report on the σ_{em} values for electronically excited ions produced by the $He(2^3S)$ Penning ionization of CO_2, CS_2, OCS, N_2O, C_6F_6, and C_6F_5H and partial σ_{em}'s for the vibrational bands of the $OCS^+(\tilde{A}^2\Pi–\tilde{X}^2\Pi)$ system produced from OCS. Moreover, the interaction potentials between $He(2^3S)$ and triatomic molecules above thermal energy have been discussed on the basis of the dependence of σ_{em} on the relative collision energy.

Experimental

The apparatus and experimental details concerning the fluorescence measurement were previously reported.[6,20] In brief, $He(2^3S, 2^1S)$ atoms are produced with a nozzle discharge source[11] and skimmed into a collision chamber; the singlet component of the total He* flux was estimated to be about 10%. The target gases flowed out to the collision chamber forming an effusive molecular beam through a multicapillary array. Under typical stable operating conditions, the discharge current was 8—25 mA, the voltage was

400—900 V, and the pressure of residual gas at the collision chamber measured by an ionization vacuum gauge was 2.7 mPa. The sample gases of N_2, CO_2, and N_2O were used without further purification, while CS_2, C_6F_6, and C_6F_5H were used after degassing. The sample of OCS was vacuum distilled prior to use in order to eliminate any CO_2 impurity.

The fluorescence resulting from the collision of He(2^3S) with the target molecules was observed in a direction perpendicular to both the molecular and He* beams. The relative sensitivity of the total photon-detection system was calibrated with a deuterium lamp in the 200—310 nm region and with a halogen lamp in the 310—650 nm region. In the present study, the σ_{em} for the fluorescence produced by collisions of He(2^3S) was evaluated by comparing its emission intensity with that of the following Penning ionization.

$$He(2^3S) + N_2 \rightarrow N_2^+(B^2\Sigma_u^+) + He + e. \quad (1)$$

We adopted a σ_{em} value of $(3.2\pm0.3)\times10^{-20}$ m^2 for reaction 1 at a relative collision energy (E_R) of 140 meV; this value was estimated from Fig. 5 in Ref. 7. The total emission intensity of the N_2^+(B–X) system was derived from the intensities of the 0–0 and 1–0 bands using the scaling factors calculated by Comes and Speier.[21] The density and spatial distribution of the target molecules at the collision region were calibrated from the target pressure measured with an MKS Baratron by a similar method to that previously reported.[22]

The velocity distributions of the He* beam measured with a separate apparatus equipped with a similar He* beam source.[20] The velocity distribution of the He* beam was obtained by measuring the time of flight (TOF) from the chopper disk to a plate (stainless steel) placed 810 mm downstream in the metastable atom detection chamber. The TOF spectrum was recorded by a digital oscilloscope with a channel width of 1 μs, and was accumulated with a personal computer. The average kinetic energy (E_M) of the He* beam, which was derived from the root-mean-square velocity (v_M) of the He* beam, was found to depend only on the discharge power at the beam source.[20]

In the fluorescence measurements, we did not use the chopped He* beam because of the weak fluorescence intensity. Thus, we controlled the kinetic energy of the He* beam by varying the discharge power, since E_M increases with the discharge power; the kinetic-energy distribution of the He* beam was estimated to be 40 meV (hwhm) at E_M=120 meV and 80 meV at 200 meV. Therefore, it should be stressed that the σ_{em} values were measured by the He* beam with relatively broad collision energies.

The relative velocity averaged over the velocities of the He* atoms and the target molecules is expressed as

$$v_R = (v_M^2 + 3kT/m)^{1/2}, \quad (2)$$

where T and m are the temperature (300 K) and the mass of the target molecule, respectively. The collision energy dependence of σ_{em} was obtained by converting the function of E_M into that of E_R with a relation between E_R and the reduced mass (μ) of the He+target system,

$$E_R = \mu v_R^2/2. \quad (3)$$

Calculations

In order to discuss the observed results concerning the collision energy dependence of the σ_{em}'s for the $CS_2^+(\tilde{A}^2\Pi_u–\tilde{X}^2\Pi_g, \tilde{B}^2\Sigma_u^+–\tilde{X}^2\Pi_g)$ band, the interaction potential curves for a He(2^3S) atom approaching carbon and sulfur atoms along several directions were calculated for CS_2 using ab initio molecular orbital (MO) methods. Since there are difficulties associated with calculating the excited states and a well-known resemblance between He(2^3S) and Li(2^2S), in this study a Li(2^2S) atom was used in place of He(2^3S).[11,23,24] It has been shown that the interaction potential well depths and the location of the potential wells have also been found to be very similar for the interactions of various targets with He(2^3S) and Li(2^2S).[1,25,26]

The interaction potentials between a Li(2^2S) atom and CS_2 were calculated using the Gaussian 94 program package[27] in an unrestricted Hartree–Fock scheme and the Moller–Plesset perturbation method (MP2). The nuclear positions of CS_2 were fixed at the experimental geometries.[28] Potential-energy curves for various directions were obtained as functions of the distance (R) between the Li atom and the center of CS_2. Ohno and Sunada[23] studied the basis-set dependences of the potential energy curves for some simple molecules. On the basis of their results, the standard 4-31G* basis sets were employed with a diffuse function for negative ions (C, S, Li).[29] The resulting basis set is denoted as 4−31+G*.

Results and Discussion

Emission Spectra Figure 1 displays a fluorescence spectrum in the 280—500 nm region produced by the He(2^3S) Penning ionization of CO_2 at 146 meV. The spectrum consists of the $CO_2^+(\tilde{A}^2\Pi_u–\tilde{X}^2\Pi_g)$ and $CO_2^+(\tilde{B}^2\Sigma_u^+–\tilde{X}^2\Pi_g)$ transitions. The vibrational bands were assigned with the aid of previous spectra.[13,30]

Figure 2 shows an emission spectrum in the 240—600 nm region resulting from collision of CS_2 with He(2^3S). The observed emission systems were identified on the basis of the previous spectra.[14,15] In this experiment the CS($A^1\Pi–X^1\Sigma^+$) emission at 260 nm was very weak, while this band in the 240—330 nm region was very intense in the FA measurements;[14,15] in the latter case, CS(A) is mainly produced via an electron recombination reaction with $CS_2^+(\tilde{X})$.[14b] Such a recombination reaction is negligible under the present experimental conditions. The emission intensity of the $CS_2^+(\tilde{B}^2\Sigma_u^+–\tilde{X}^2\Pi_g)$ system was evaluated in the 278—293 nm region, while the emission intensity of the $CS_2^+(\tilde{A}^2\Pi_u–\tilde{X}^2\Pi_g)$ system in the 400—600 nm region overlaps with the $CS^+(A^2\Pi_i–X^2\Sigma^+)$ band at wavelengths longer than 520 nm, and with a structureless emission in the 300—520 nm region; these bands are indicated by the broken lines in Fig. 2. Yencha and Wu[15] also reported such a continuous band in the 310—475 nm region, which is attributable to a neutral CS_2 fluorescence. Although we do not specify the emitter, we cannot accept the formation of such a neutral emitter under the present experimental condition.

Figure 3 shows the emission spectrum in the 300—540 nm region resulting from the reaction of OCS with He(2^3S). Many emission bands, which were very weak, are assigned to the $OCS^+(\tilde{A}^2\Pi–\tilde{X}^2\Pi)$ and $CO^+(A^2\Pi_i–X^2\Sigma^+)$ systems.[17,18,31,32] The $OCS^+(\tilde{A}–\tilde{X})$ emission consists of the $3^0_{v''}$ bands for v''=0—6. The absence of fluorescence from the vibrational excited levels is ascribed to predissociation into $CO(X^1\Sigma^+)+S(^4S_u \text{ or } ^2D_u)^+$.[33] The vibrational levels of

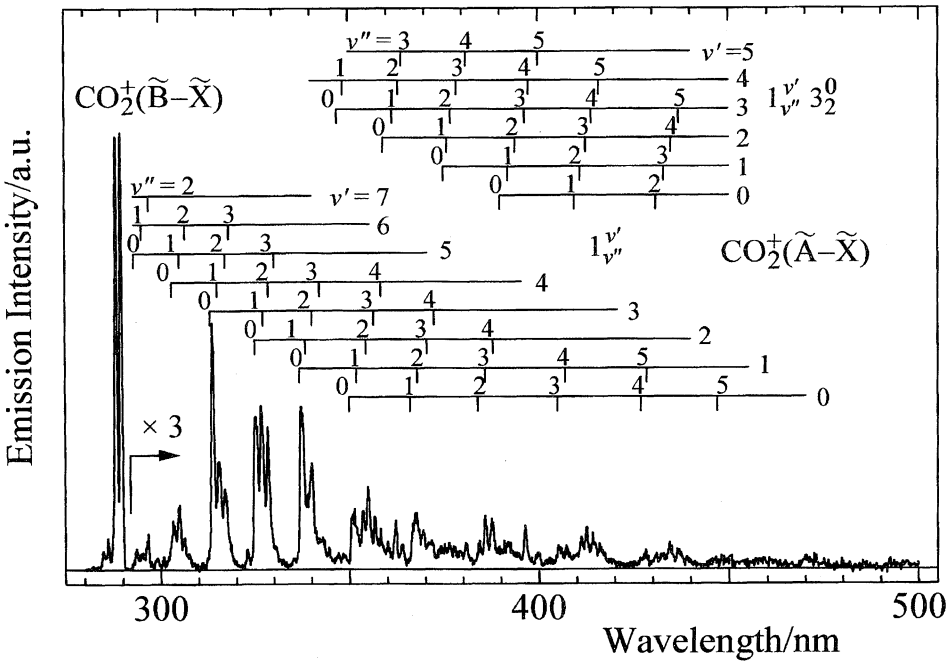

Fig. 1. A typical emission spectrum resulting from collision of He(2^3S) with CO_2 measured at E_R of 146 meV with the optical resolution of 0.6 nm (fwhm); the optical sensitivity is calibrated.

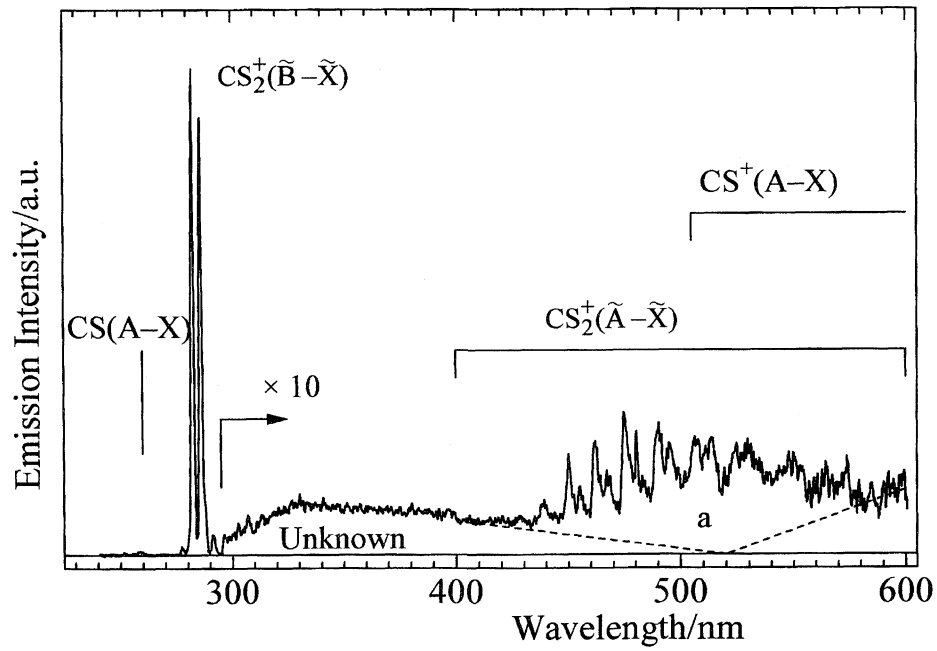

Fig. 2. Same as Fig. 1 but for CS_2 measured at E_R of 150 meV with the optical resolution of 1.5 nm (fwhm): the area bounded by the broken lines (area a) is assumed to be the $CS_2^+(\tilde{A}-\tilde{X})$ emission for evaluating σ_{em}.

the $CO^+(A^2\Pi, v')$ state for v' up to 5 have been observed from the $CO^+(A^2\Pi_i-X^2\Sigma^+)$ emission. However, the $v' \geq 1$ levels of the $CO^+(A)$ state are energetically impossible to be directly produced by the dissociative ionization of OCS with He(2^3S: 19.82 eV), since the threshold energy for the reaction of $OCS \rightarrow CO^+(A^2\Pi)+S(^3P)$ is estimated to be 19.74±0.01 eV from related data.[34,35] Thus, the helium metastable atom, He(2^1S: 20.62 eV), mixed about 10% in a He* beam seems to be a candidate for the excitation source.

Figure 4 shows the emission spectra in the 400—650 nm region resulting from the collision of C_6F_6 and C_6F_5H with He(2^3S). The $C_6F_6^+(\tilde{B}-\tilde{X})$ emission from C_6F_6 and the $C_6F_5H^+(\tilde{B}-\tilde{X}, \tilde{B}-\tilde{A})$ emission from C_6F_5H were assigned on the basis of published data.[36,37]

Emission Cross Sections. Table 1 lists the σ_{em} values obtained for several transitions compared with those estimated from the emission rate constants measured by the FA method;[12,13,18,19] the uncertainty attached to the σ_{em} values in this study includes both the uncertainty (9%) in the σ_{em} value for the reference reaction and the experimental errors (3—

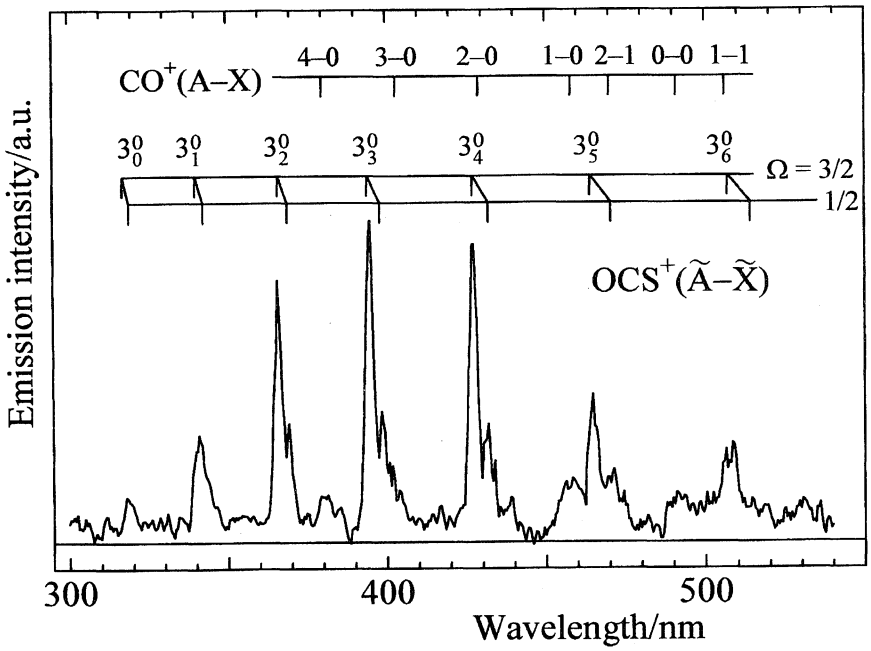

Fig. 3. Same as Fig. 2 but for OCS measured at E_R of 148 meV.

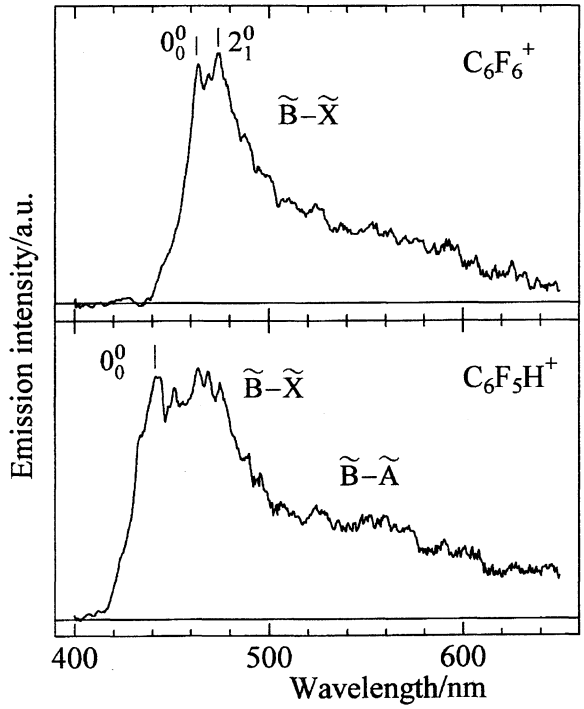

Fig. 4. Same as Fig. 2 but for C_6F_6 and C_6F_5H measured at E_R of 155 meV.

10%). The values obtained in this study appear to be slightly smaller than the thermal data. This probably originates in the fact that the σ_{em} value of $(3.2\pm0.3)\times10^{-20}$ m^2 adopted for reaction 1 is rather small. On the other hand, the value of the partial cross section for $N_2^+(B)$ in reaction 1 can be estimated to be $(5.2\pm1.3)\times10^{-20}$ m^2 at 140 meV from Table 3 in Ref. 11. The latter value, however, seems to be fairly large.

The σ_{em} values for the $CO_2^+(\tilde{A}–\tilde{X})$ and $CO_2^+(\tilde{B}–\tilde{X})$ systems produced by the He(2^3S) Penning ionization of CO_2 at 146 meV were evaluated to be 10.3±1.5 and 4.3±0.6, respectively, in units of 10^{-20} m^2, which roughly agree with the previous values[12,13] measured at the thermal energy. Nevertheless, the ratio of σ_{em} for the $\tilde{A}$ state to that for the $\tilde{B}$ state, $\sigma_{em}(A)/\sigma_{em}(B)$, derived in this study (at 146 meV) is 2.4±0.4, which is smaller than the value of 3.7 obtained at the thermal energy.[13]

It is well-known that the σ_{em}'s for the A and B states of CO_2^+ derived from fluorescence experiments are enhanced by internal conversion from the B state to the A state; the crossover ratio was evaluated to be 0.55 from the fluorescence excitation and photoelectron spectra[38] and 0.46 from a photon-photoion coincidence method.[39] Thus, the partial cross sections for the A and B states of CO_2^+ and the branching ratios of the A and B states (*A*/*B*) are estimated from the PIOS data on the assumption of a 50% crossover. The thus-obtained partial cross sections of the A and B states are 6.0 and 8.6×10^{-20} m^2, respectively, based on the assumption of a fluorescence quantum yield of unity for $CO_2^+(\tilde{A}$ plus $\tilde{B})$.[39] The $\sigma_{em}(A)/\sigma_{em}(B)$ and *A*/*B* ratios resulting from the He(2^3S) Penning ionization of CO_2 are summarized in Table 2. The partial cross section of $CO_2^+(\tilde{A})$ increases greatly with the collision energy, whereas that of $CO_2^+(\tilde{B})$ is nearly constant in the 60—400 meV region.[11] Thus, the *A*/*B* ratio increases with the collision energy. The ratio of 0.7±0.2 derived in this experiment, however, is slightly smaller than the values by PIES.[3,10,11] This result indicates that the crossover ratio is smaller than 0.50 at a collision energy of 100—200 meV; if we dare to say, it is 0.40—0.45. On the other hand, the *A*/*B* value obtained by Endoh et al.[13] seems to be larger than the PIES's values. The discrepancy between our ratio and that of Endoh et al. is probably caused by corrections for the relative sensitivity of the photon-detection system.

The σ_{em} for the $CS_2^+(\tilde{B}–\tilde{X})$ system produced by the

Table 1. σ_{em} Values for Several Transitions Resulting from He(2^3S) Penning Ionization of Simple Molecules

Transition	Method[a]	σ_{em} / 10^{-20}m^2	E_R/meV	Ref.
$CO_2^+(\tilde{A}^2\Pi_u-\tilde{X}^2\Pi_g)$	FA	12.0±6.3[b]	57—72	12
	FA	14.0±1.4[b]	57—72	13
	CB	10.3±1.5	146±57[c]	This work
$CO_2^+(\tilde{B}^2\Sigma_u^+-\tilde{X}^2\Pi_g)$	FA	7.7±3.5[b]	57—72	12
	FA	3.9±0.4[b]	57—72	13
	CB	4.3±0.6	146±57[c]	This work
$CS_2^+(\tilde{A}^2\Pi_u-\tilde{X}^2\Pi_g)$	CB	1.4±0.3	150±57[c]	This work
$CS_2^+(\tilde{B}^2\Sigma_u^+-\tilde{X}^2\Pi_g)$	CB	2.8±0.3	150±57[c]	This work
$OCS^+(\tilde{A}^2\Pi-\tilde{X}^2\Pi)$	FA	0.040±0.004	57—72	18
	CB	0.031±0.004	148±57[c]	This work
$N_2O^+(\tilde{A}^2\Sigma^+-\tilde{X}^2\Pi)$	CB	4.2±0.4	146±57[c]	This work
$C_6F_6^+(\tilde{B}^2A_{2u}-\tilde{X}^2E_{1g})$	FA	1.5[b]	40	19
	CB	0.72±0.11	155±57[c]	This work
$C_6F_5H^+(\tilde{B}^2A_1-\tilde{X}^2B_1)$	FA	1.3[b]	40	19
	CB	0.73±0.11	155±57[c]	This work

a) CB: crossed beam; FA: flowing afterglow. b) The σ_{em}'s evaluated from the formation rate constants assuming 300 K. c) Uncertainties represent the spread (hwhm) in the kinetic energy distribution for the He* beam.

Table 2. The $\sigma_{em}(A)/\sigma_{em}(B)$ and A/B rations of CO_2^+ Produced from He(2^3S) Penning Ionization of CO_2 Measured by PIES and PIOS

Method	E_R/meV	$\sigma_{em}(A)/\sigma_{em}(B)$	A/B	Ref.
PIOS	57—72	1.6±1.1	0.28[b]	12a
PIOS	57—72	3.7±0.7	1.35±0.35[b]	13
PIOS	146±57[a]	2.4±0.4	0.7±0.2[b]	This work
PIES	72—90		0.88± 0.20	10
PIES	72		1.03± 0.15	3
	200		1.62± 0.25	
PIES	70		0.66± 0.14	11
	120		0.90± 0.19	
	200		1.21± 0.20	

a) Uncertainty represent the spread (hwhm) in the kinetic energy distribution for the He* beam. b) Evaluated on the assumption of a 50% crossover from the B state to the A state.

He(2^3S) Penning ionization of CS_2 was evaluated to be $(2.8\pm0.3)\times10^{-20}$ m^2. For the $CS_2^+(\tilde{A}-\tilde{X})$ emission in the 400—600 nm region, the area bounded by the broken lines (area a) is regarded as the most probable intensity for the $CS_2^+(\tilde{A}-\tilde{X})$ system because of overlapping with the unknown broad band and with the CS^+(A–X) emission, as described in the previous section; the total intensity in the 400—600 nm region is assumed to be the upper limit of the emission intensity for the $CS_2^+(\tilde{A}-\tilde{X})$ band. The thus-evaluated σ_{em} for the $CS_2^+(\tilde{A}-\tilde{X})$ system is $(1.4\pm0.3)\times10^{-20}$ m^2 (see Table 1). The partial cross section of $CS_2^+(\tilde{B})$ can be evaluated from the fluorescence quantum yield of 0.37±0.04,[39] while the fluorescence quantum yield for $CS_2^+(\tilde{A})$ has not been determined because of its long lifetime.

For the $OCS^+(\tilde{A}-\tilde{X})$ system, the 3_4^0 band is found to be overlap with the 2–0 band of the CO^+(A–X) system. Thus, the intensity of the 3_4^0 band was evaluated by subtracting that of the 2–0 band; the latter was estimated from the observed intensities of the 0–0, 1–0, 3–0, and 4–0 bands and the Einstein A coefficients calculated for the CO^+(A–X) system.[40] The partial σ_{em}'s and band strengths of the $3_{v''}^0$ bands for v''=0—6 are listed in Table 3 along with the data obtained by the photoionization of OCS;[31] the band strengths (P) correspond to the experimental Franck–Condon factors of the $OCS^+(\tilde{A}-\tilde{X})$ transition. The present result is slightly different from the data measured by Judge and Lee.[31] This discrepancy is probably caused by an overlapping of the emissions which were assigned as the $1_1^0 3_{v''}^0$ and $1_2^0 3_{v''}^0$ bands (Fig. 1 in Ref. 31). In the present data, these combination bands appear to be very weak.

The total σ_{em} for the $OCS^+(\tilde{A}-\tilde{X})$ system resulting from the He(2^3S) Penning ionization of OCS is evaluated to be $(0.031\pm0.004)\times10^{-20}$ m^2 (see Table 1). This is in reasonable agreement with the value measured by the FA method.[18] The partial cross section for the formation of $OCS^+(\tilde{A})$ from

Table 3. Partial σ_{em} and Band Strengths (P) for the Vibrational Bands of the $OCS^+(\tilde{A}^2\Pi-\tilde{X}^2\Pi)$ System

Band	λ[c] / nm	PIOS[a] σ_{em} / 10^{-22}m^2	PIOS[a] P	Photoionization[b] P Ω=1/2	Photoionization[b] P 3/2
3_0^0	318.95	0.09(6)	0.06(2)		
3_1^0	341.47	0.33(11)	0.28(1)		
3_2^0	366.83	0.65(21)	0.71(2)	0.48	0.55
3_3^0	395.59	0.73(24)	1.00	1.00	1.00
3_4^0	428.34	0.60(21)	1.03(3)	0.99	1.07
3_5^0	466.05	0.42(13)	0.93(2)	0.89	0.82
3_6^0	509.91	0.24(11)	0.69(3)		

a) An average for the Ω=1/2 and 3/2 components obtained in this work; numbers in parentheses represent the errors attached to the last digits. b) Ref. 31. c) Statistically weighted wavelengths for the Ω=1/2 and 3/2 components.

OCS can be estimated on the basis of the fluorescence quantum yield, 0.17±0.04, for the 3^0 level of the $OCS^+(\tilde{A})$ state,[41] and the Franck–Condon factor (0.05±0.01) observed for the 3_0^0 band of the $OCS^+(\tilde{A}) \leftarrow OCS(\tilde{X})$ excitation.[42] The thus-estimated partial cross section of $OCS^+(\tilde{A})$ from OCS is $(3.6\pm0.5)\times10^{-20}$ m^2.

The σ_{em} value of $(4.2\pm0.4)\times10^{-20}$ m^2 for the $N_2O^+(\tilde{A}^2\Sigma^+-\tilde{X}^2\Pi)$ band produced by the He(2^3S) Penning ionization of N_2O becomes half of the value $(8.0\pm2.1)\times10^{-20}$ m^2 reported in a preliminary paper.[6] In the present study, the other σ_{em} value[7] for reference reaction 1 is adopted, as mentioned above, and density and spatial distribution of the target molecules in the effusive beam were calibrated.

The σ_{em}'s for $C_6F_6^+(\tilde{B}^2A_{2u}-\tilde{X}^2E_{1g})$ and $C_6F_5H^+(\tilde{B}^2A_1-\tilde{X}^2B_1)$ in the 400—650 nm region were evaluated to be 0.72±0.11 and $(0.73\pm0.11)\times10^{-20}$ m^2, respectively; the value for the $C_6F_5H^+(\tilde{B}-\tilde{X})$ system includes the contribution of the $C_6F_5H^+(\tilde{B}-\tilde{A})$ emission overlapped above 540 nm. These σ_{em} values are fairly smaller than those obtained at the thermal energy.[19] This difference can be explained by the fact that the partial cross section of the $a_{2u}(\pi)$ band for benzene is PIES decreases with increasing with the collision energy in the 60—200 meV range;[43] the collision energy dependence of the partial cross section for the $\tilde{B}^2A_{2u}$ $(a_{2u})^{-1}$ state of $C_6F_6^+$ is expected to be similar to that for benzene.

Collision Energy Dependence of σ_{em}. In the Penning ionization of the He* atom with Ar at very low energies, the total and state-resolved ionization cross sections (σ) decrease as the collision energy increases until about 100 meV, where they begin to rise.[8b,44] As the collision energy increases, the cross section reaches a maximum at around 10 eV. The first decrease originates in the long-range attractive potential. When the effective potential $V^*(R)$ is represented by

$$V^*(R) \propto -R^{-s}, \tag{4}$$

$\sigma(E)$ can be expressed by

$$\sigma(E) \propto E^{-2/s}. \tag{5}$$

In the second increase region, the repulsive part of the interaction potential governs the energy dependence. From the simple theoretical consideration,[45] $\sigma(E)$ can be represented by

$$\sigma(E) \propto E^{b/d-1/2}, \tag{6}$$

neglecting the minor dependence on the collision energy. The parameter d represents the effective hardness of the repulsive potential of the form

$$V^*(R) \propto \exp(-dR), \tag{7}$$

and b expresses the transition probability of the simple analytical form

$$W(R) \propto \exp(-bR). \tag{8}$$

By comparing Eqs. 5 and 6, it is concluded that the dependence of σ_{em} on the collision energy can be expressed by the slope (m) over a wider energy range, where the effective potential is whether attractive or repulsive. Figure 5 shows $\log \sigma_{em}(E_R)$ vs. $\log E_R$ plots for ions produced by Penning ionization. The m values obtained by a least-square method are listed in Table 4 along with the data obtained by PIES.[7,11,46] In the He(2^3S) Penning ionization of simple molecules, many data on the collision-energy dependence of the partial cross section for ions were accumulated by PIES,[11,36,46,47] while there are only a few data on the collision-energy dependence of σ_{em}'s for ions measured by PIOS.[7] The m value obtained for $N_2^+(B)$, which is in reasonable agreement with the data by PIOS,[7] is apparently smaller than that obtained by PIES.[11] In the PIOS study He(2^1S) is mixed about 10% in the He* beam, whereas the singlet component is quenched by a helium lamp in the PIES study. Nevertheless, the total cross section, theoretically calculated on the He(2^1S)+Ar ionization, depends on the collision energy in the same feature as that for the He(2^3S)+Ar ionization.[8b] It is thus expected that the influence of He(2^1S) on the m value is negligible. The difference between our data and the PIES's data originates in the fact that the collision energy region used in this study was higher than those used in PIES, since the partial cross section for $N_2^+(B)$ steeply increases with the collision energy at a lower region, and appears to reach a maximum at around 400 meV.[11] The difference also appears

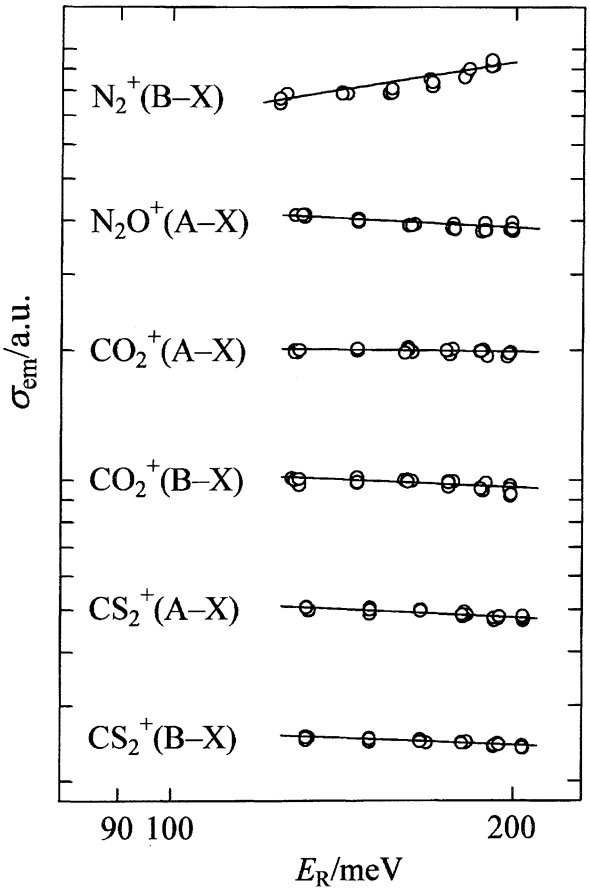

Fig. 5. $\log \sigma_{em}(E_R)$ vs. $\log E_R$ plots for several emissions produced by He(2^3S) Penning ionization.

Table 4. Slope Parameter m Determined from log $\sigma_{em}(E_R)$ vs. log E_R Plots

Target	Ion state	m[a]	E_R/meV	Method	Ref.
N_2	$B^2\Sigma_u^+$	1.21(7)	60—100	PIES	11
		0.61(5)[b]	80—140	PIOS	7
		0.42(8)	125—190	PIOS	This work
N_2O	$\tilde{A}^2\Sigma^+$	−0.11(3)	80—250	PIES	46
		−0.14(6)	130—200	PIOS	This work
CO_2	$\tilde{A}^2\Pi_u$	0.59(9)	60—400	PIES	11
		0.20(3)	100—400	PIES	46
		−0.03(5)	130—200	PIOS	This work
	$\tilde{B}^2\Sigma_u^+$	0.012(8)	60—400	PIES	11
		−0.23(3)	100—400	PIES	46
		−0.12(5)	130—200	PIOS	This work
CS_2	$\tilde{A}^2\Pi_u$	−0.13(5)	130—205	PIOS	This work
	$\tilde{B}^2\Sigma_u^+$	−0.11(5)	130—205	PIOS	This work

a) Numbers in parentheses represent the errors attached to the last digits. b) Estimated from Fig. 6 in Ref. 7.

in the m value for $CO_2^+(\tilde{A})$; the m value for $CO_2^+(\tilde{A})$ obtained in this study is more negative than the value remeasured by Ohno et al.[46] Although we cannot clearly explain the trend, the log $\sigma(E)$ vs. log E plots for $CO_2^+(\tilde{A})$ seem to deviate from linearity in the 60—400 meV range (Figs. 2 and 3 in Ref. 11). Therefore, the m values obtained in this study are probably affected by the contribution from the upper or lower part of the collision energy, since the kinetic-energy distribution of the He* beam was fairly broad. On the other hand, the m values for $N_2O^+(\tilde{A}^2\Sigma^+)$ and $CO_2^+(\tilde{B})$ are consistent with the PIES's values. The m values obtained for the $\tilde{A}^2\Pi_u$–$\tilde{X}^2\Pi_g$ and $\tilde{B}^2\Sigma_u^+$–$\tilde{X}^2\Pi_g$ bands of CS_2^+ are slightly negative. This indicates that the effective potentials are slightly attractive.

Ohno and his co-workers studied the interaction potentials between He(2^3S) and N_2,[11,23,46] CO_2,[11,23,46] and N_2O[46] by ab initio MO methods. Thus, we shall confine ourselves to the result for the interaction potential between He(2^3S) and CS_2. Figure 6 shows the potential-energy curves $V(R, \theta)$ obtained from the model potential calculations between He(2^3S)/Li(2^3S) and CS_2. The potential curves obtained in the HF scheme are approximately single exponential functions, whereas those by MP2 perturbation method exhibit a considerable downward deformation from the exponential type. The curves in the HF results are best-fitted single exponential functions (Eq. 7); the d values in atomic units are 1.09 for θ=0° and 0.90 for θ=90°. The HF results up to 200 meV show that the repulsive well for an end-on approach (θ=0°) is harder than that for a side-on approach (θ=90°). This trend is similar to those for CO_2.[11] Nevertheless, a very shallow well (50 meV) can be seen for the end-on approach in the case of CO_2.[11] Such a well does not appear in the HF curves for CS_2, whereas the MP2 results for CS_2 exhibit a considerable downward deformation, and then show a very shallow well near 0.4 nm for a side-on approach. The MP2 curves for CS_2 are harder than the corresponding the HF curves. The angular dependence of the potential-energy curves for CS_2

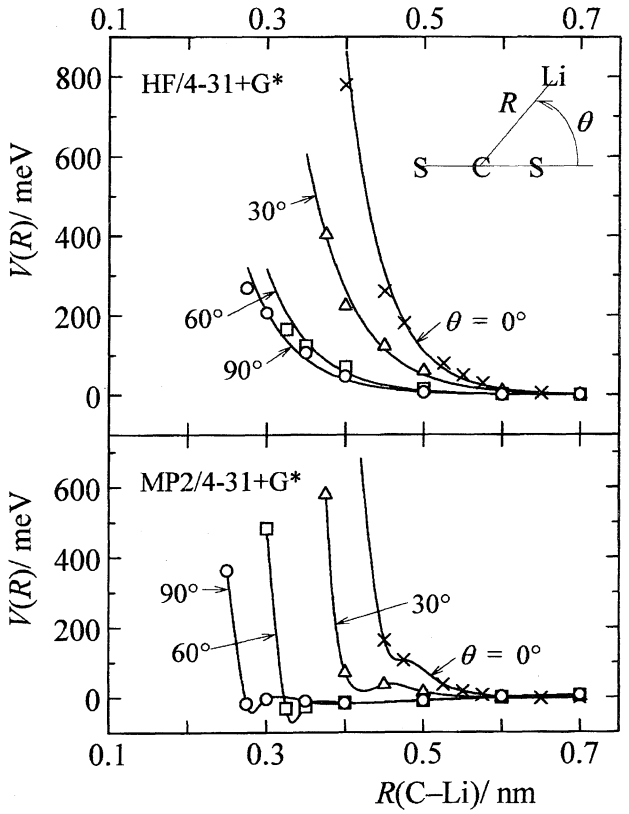

Fig. 6. Model potential curves $V(R, \theta)$ for CS_2–He*. In place of He(2^3S), Li(2^2S) is used for the calculation. R is the distance between Li and the center of mass for CS_2, and θ is the angle from the collinear axis; (×) for θ=0°, (△) for θ=30°, (□) for θ=60°, (○) for θ=90°.

obtained by MP2 calculations in Fig. 6 indicates a general feature of the molecular surface on going from an attractive well to a repulsive well. These features of the MP2 results are consistent with the slightly negative m values for the $\tilde{A}$–$\tilde{X}$ and $\tilde{B}$–$\tilde{X}$ bands of CS_2^+.

In summary, the σ_{em} values for several ion states were determined, for the first time, at a higher energy region by PIOS. The collision energy dependence of σ_{em} for ionic species can provide semiquantitative information on the interaction potentials between He(2^3S) and the target molecules.

We are grateful to Dr. M. Tsuji of Kyushu University for fruitful discussions. We are also indebted to Prof. K. Ohno and to Dr. H. Yamakado of Tohoku University for providing PIES data and for helpful suggestions on the ab initio MO calculation. This work was partly supported by a Grand-in-Aid for Scientific Research No. 07454149 from the Japanese Ministry of Education, Science and Culture.

References

1) A. Niehaus, *Adv. Chem. Phys.*, **45**, 399 (1981).
2) V. Cermák, *J. Chem. Phys.*, **44**, 3781 (1966).
3) H. Hotop, E. Kolb, and J. Lorenzen, *J. Electron Spectrosc. Relat. Phenom.*, **16**, 213 (1979).
4) W. W. Robertson, *J. Chem. Phys.*, **44**, 2456 (1966).

5) D. H. Stedman and D. W. Setser, *Prog. React. Kinet.*, **6**, 193 (1971).
6) I. Tokue, T. Kudo, and Y. Ito, *Chem. Phys. Lett.*, **199**, 435 (1992).
7) R. A. Sanders, A. N. Schweid, M. Weiss, and E. E. Muschlitz, Jr., *J. Chem. Phys.*, **65**, 2700 (1976).
8) a) J. T. Moseley, J. R. Peterson, D. C. Lorents, and M. Hollstein, *Phys. Rev. A*, **A6**, 1025 (1972); b) R. E. Olson, *Phys. Rev. A*, **A6**, 1031 (1972).
9) V. Cermák, *J. Electron Spectrosc. Relat. Phenom.*, **9**, 419 (1976).
10) C. E. Brion and D. S. C. Yee, *J. Electron Spectrosc. Relat. Phenom.*, **12**, 77 (1977).
11) K. Ohno, T. Takami, K. Mitsuke, and T. Ishida, *J. Chem. Phys.*, **94**, 2675 (1991).
12) a) T. S. Wauchop and H. P. Broida, *J. Quant. Spectrosc. Radiat. Transfer*, **12**, 371 (1972); b) G. Taib and H. P. Broida, *Chem. Phys.*, **21**, 313 (1977).
13) M. Endoh, M. Tsuji, and Y. Nishimura, *J. Chem. Phys.*, **77**, 4027 (1982).
14) a) J. A. Coxon, P. J. Marcoux, and D. W. Setser, *Chem. Phys.*, **17**, 403 (1976); b) P. J. Marcoux, M. van Swaay, and D. W. Setser, *J. Phys. Chem.*, **83**, 3168 (1979).
15) A. J. Yencha and K. T. Wu, *Chem. Phys.*, **49**, 127 (1980).
16) D. Cossart, *J. Chim. Phys.*, **78**, 711 (1981).
17) D. W. Setser, *Int. J. Mass Spectrom. Ion Phys.*, **11**, 301 (1973).
18) M. Tsuji, M. Matsuo, and Y. Nishimura, *Int. J. Mass Spectrom. Ion Phys.*, **34**, 273 (1980).
19) R. S. F. Chang, D. W. Setser, and G. W. Taylor, *Chem. Phys.*, **25**, 201 (1978).
20) I. Tokue, Y. Sakai, M. Kobayashi, and K. Yamasaki, *Bull. Chem. Soc. Jpn.*, **69**, 2815 (1996).
21) F. J. Comes and F. Speier, *Chem. Phys. Lett.*, **4**, 13 (1969).
22) I. Tokue, M. Kudo, M. Kusakabe, T. Honda, and Y. Ito, *J. Chem. Phys.*, **96**, 8889 (1992).
23) K. Ohno and S. Sunada, *Proc. Indian Acad. Sci.*, **106**, 327 (1994).
24) H. Yamakado, M. Yamaguchi, S. Hoshino, and K. Ohno, *J. Phys. Chem.*, **99**, 17096 (1995).
25) H. Hotop, *Radiat. Res.*, **59**, 379 (1974).
26) H. Haberland, Y. T. Lee, and P. E. Siska, *Adv. Chem. Phys.*, **45**, 487 (1981).
27) M. J. Frisch, G. W. Trucks, H. B. Schlegel, P. M. W. Gill, B. G. Johnson, M. A. Robb, J. R. Cheeseman, T. Keith, G. A. Petersson, J. A. Montgomery, K. Raghavachari, M. A. Al-Laham, V. G. Zakrzewski, J. V. Ortiz, J. B. Foresman, C. Y. Peng, P. Y. Ayala, W. Chen, M. W. Wong, J. L. Andres, E. S. Replogle, R. Gomperts, R. L. Martin, D. J. Fox, J. S. Binkley, D. J. Defrees, J. Baker, J. P. Stewart, M. Head-Gordon, C. Gonzalez, and J. A. Pople, "Gaussian 94, Revision B. 2," Gaussian, Inc., Pittsburgh, PA (1995).
28) A. G. Maki and R. L. Sams, *J. Mol. Spectrosc.*, **52**, 233 (1974).
29) W. J. Hehre, L. Radom, P. V. R. Schleyer, and J. A. Pople, "Ab initio Molecular Orbital Theory," John Wiley and Sons, New York (1986).
30) I. Tokue, H. Shimada, A. Masuda, Y. Ito, and K. Kume, *J. Chem. Phys.*, **93**, 4812 (1990).
31) D. L. Judge and L. C. Lee, *Int. J. Mass Spectrom. Ion Phys.*, **17**, 329 (1975).
32) R. W. Nicholls, *Can. J. Phys.*, **40**, 1772 (1962).
33) a) J. H. D. Eland, *Int. J. Mass Spectrom. Ion Phys.*, **12**, 389 (1973); b) B. Brehm, R. Frey, A. Küstler, and J. H. D. Eland, *Int. J. Mass Spectrom. Ion Phys.*, **13**, 251 (1974).
34) M. W. Chase, Jr., C. A. Davies, J. R. Downey, Jr., D. J. Frurip, R. A. McDonald, and A. N. Syverud, *J. Phys. Chem. Ref. Data*, **14**, Suppl. No. 1 (1985).
35) K. P. Huber and G. Herzberg, "Molecular Spectra and Molecular Structure, Vol. 4, Constants of Diatomic Molecules," Van Nostrand-Reinhold, New York (1979).
36) V. E. Bondybey and T. A. Miller, *J. Chem. Phys.*, **70**, 138 (1979); **73**, 3053 (1980).
37) M. Allan, J. P. Maier, and O. Marthaler, *Chem. Phys.*, **26**, 131 (1977).
38) J. A. R. Samson and J. L. Gardner, *J. Geophys. Res.*, **78**, 3663 (1973).
39) J. H. D. Eland, M. Devoret, and S. Leach, *Chem. Phys. Lett.*, **43**, 97 (1976).
40) D. C. Jain, *J. Phys. B*, **B5**, 199 (1972).
41) J. P. Maier and F. Thommen, *Chem. Phys.*, **51**, 319 (1980).
42) D. C. Frost, S. T. Lee, and C. A. McDowell, *J. Chem. Phys.*, **59**, 5484 (1973).
43) T. Takami and K. Ohno, *J. Chem. Phys.*, **96**, 6523 (1992).
44) A. Niehaus, *Ber. Bunsenges. Phys. Chem.*, **77**, 632 (1973).
45) E. Illenberger and A. Niehaus, *Z. Phys. B*, **B20**, 3590 (1975).
46) K. Ohno et al., to be published.
47) K. Mitsuke, T. Takami, and K. Ohno, *J. Chem. Phys.*, **91**, 1618 (1989).